J Electroceram (2007) 18:269–276
DOI 10.1007/s10832-007-9127-1

Glass-ceramics of barium strontium titanate for high energy density capacitors

E. P. Gorzkowski · M.-J. Pan · B. Bender · C. C. M. Wu

Received: 13 September 2006 / Accepted: 5 April 2007 / Published online: 1 May 2007

Abstract Barium strontium titanate glass-ceramics were successfully produced with one major crystalline phase when Al_2O_3 was added to the melt. A dielectric constant of 1000 and a breakdown strength of 800 kV/cm was achieved; however the energy density was only measured to be 0.3–0.9 J/cm^3. These energy density values were lower than anticipated due to the presence of dendrites and pores in the microstructure. Using BaF_2 as a refining agent improved the microstructure and doubled the energy density for BST 80/20 samples. However, no refining agent reduced the increasing amount of hysteresis that developed with increasing applied electric field. This phenomenon is believed to be due to interfacial polarization.

Keywords Glass-ceramic · Breakdown strength · Ferroelectric materials

1 Introduction

Currently, warships and combat vehicles are built with a propulsion system that is separate from the auxiliary systems and weapons. Therefore, a large amount of power is locked into the mechanical propulsion train and is not available for any other use. To remedy this issue the currently planned all-electric ship is to have both the propulsion system and the pulsed power weapons draw from the same energy source. This integration will significantly improve efficiency, effectiveness, and survivability while simultaneously increasing design flexibility, reducing total ownership costs, and enhancing the quality of service [1]. In the past several years, the U.S. Navy has made significant investment in the technology of power electronics for the all-electric ship. Despite the tremendous progress in the area of semiconductor switches [2], the passive components, especially capacitors, remain a limiting factor in the design of high power systems due to their low volumetric efficiency [3]. In pulsed power weapon applications, where capacitor banks can occupy many cubic meters of space, the importance of developing high energy density dielectric materials is essential.

There are several classes of materials that can be improved to develop these high-energy density capacitors, but each has limitations. Ceramics generally have a high dielectric constant, K, (~4000), but possess low breakdown strength (~100 kV/cm) [4]. Polymers on the other hand have high breakdown strength (~4000 kV/cm) but a poor dielectric constant (~3) [5]. Since the energy density is related to the product of breakdown strength squared and dielectric constant, the performance of ceramics can be improved by increasing the breakdown strength and polymers can be improved by increasing K through filler additions [6]. Consequently, improvements in breakdown strength have a more pronounced effect on the energy density so that ceramic systems have the best chance of becoming high-energy density capacitors. The low breakdown strength of ceramic capacitors is due to flaws, such as porosity, which cause electric field concentration and corona. Therefore, the energy density could easily be increased by eliminating flaws, i.e. pores, in the ceramic materials [7].

After assessing existing ceramic technologies it was found that the most attractive candidate was the develop-

E. P. Gorzkowski (✉) · M.-J. Pan · B. Bender · C. C. M. Wu
Multifunctional Materials Branch,
The Naval Research Laboratory,
Washington, DC 20375, USA
e-mail: gorzkows@anvil.nrl.navy.mil

ment of ferroelectric glass-ceramics [8]. In this approach, a glass medium comprised of glass network formers and ferroelectric constituents is prepared by melt-casting. Ferroelectric particles/grains are then precipitated within the glass matrix during subsequent heat treatment [9, 10]. The synergistic effect of good dielectric properties from the ceramic and the defect-free nature of the glass results in a material that can have high dielectric constants and high breakdown strengths [11]. The major advantage of this approach is by starting with a porosity-free glass matrix, one can eliminate the source of electric field concentration and increase the dielectric breakdown strength to the vicinity of its intrinsic value of a few MV/cm [7]. In this way, an energy density greater than one order of magnitude higher than conventional dielectrics can be achieved.

In 2003 Pennsylvania State University and the Naval Research Laboratory (NRL), completed a feasibility study that investigated the crystallization and dielectric behavior of the glass ceramics in the PbO–BaO–SrO–Nb_2O_5–B_2O_3–SiO_2 ($Sr_{0.33}Ba_{0.67}Nb_2O_6$ phase) and Na_2O–PbO–Nb_2O_5–SiO_2 ($Pb_2Nb_2O_7$, $NaNbO_3$ and $PbNb_2O_6$ phases) systems. The maximum dielectric constant, K, was approximately 250–300. The dielectric breakdown strength was 400–800 kV/cm, which is 5 to 10 times higher than conventional ceramic dielectrics [6]. Subsequently, NRL conducted an additional study using the BaO–TiO_2–Al_2O_3–SiO_2 system to produce $BaTiO_3$ as the crystalline phase. This study resulted in a K of 350 at room temperature and dielectric breakdown strengths of 600–800 kV/cm [12]. These results indicated that a final energy density of 6–8 J/cm^3 is possible, but $BaTiO_3$ exhibited inconsistency in energy density results at high field concentrations. Therefore SrO was added to the melt in order to form $Ba_{(1-x)}Sr_xTiO_3$ (BST). This allows the Curie point of the ferroelectric component of the glass-ceramic to be tailored so that the paraelectric phase can be exploited to maintain consistent dielectric properties at high field. In addition, adding strontium could potentially increase the energy density as shown by other experimental and theoretical studies [13]. This increase is necessary to achieve an energy density greater than 10 J/cm^3, which is an adequate level for a bulk material to be used on the all-electric ship. In this study, the effect of various parameters on the microstructure and dielectric properties of BST glass-ceramics is reported.

2 Experimental procedure

Barium Strontium Titanate (BST) glass was made by mixing high purity $BaCO_3$, $SrCO_3$, TiO_2, Al_2O_3, SiO_2, and refining agents such as B_2O_3, LiF, BaF_2, and P_2O_5 where indicated. The appropriate amount of each powder was added to form several batches of BST with Ba/Sr stoichiometric ratios of 0.50–0.80, while keeping the glass former content between 20 and 40 mol.%. These batches were jar milled overnight in a high density polyethylene bottle with no milling media for homogenous mixing. The powders were then placed in a platinum crucible and heated to 1500 °C in a box furnace to sequentially decompose the carbonates and to melt the constituent powders to a viscous liquid. The melt was homogenized at 1500 °C for 2 h, and then quickly removed from the furnace to be poured onto a set of rollers for quenching. Next, the transparent glass was annealed at 600 °C for 10 h to remove residual stresses. Glass from each batch was then ground using an agate mortar and pestle to a fine powder for X-ray Powder Diffraction (XRD) and DTA (Differential Thermal Analysis) measurements. The XRD was completed on a Phillips XRG 3100 diffractometer (PANalytical, The Netherlands) with Cu Kα radiation at 50 kV and 30 mA to verify that no crystallization had taken place. To determine the crystallization temperature DTA, (TA instruments, new Castle, DE) was performed using a 10 °C/min ramp rate to 1200 °C. Remaining glass from each composition was then separated into smaller lots and annealed at temperatures of 850–1200 °C in order to crystallize BST phase from the glass precursor.

One sample from each composition and heat treatment were ground into a powder with an agate mortar and pestle for XRD to verify the crystalline phases. Additional samples of each composition were prepared for dielectric testing. This entailed lapping the samples down to a thickness of ~100 μm using 400 and 600 grit SiC slurry to create flat parallel faces. Some samples were gold coated for capacitance measurements, while others were masked for breakdown and energy density measurements. The dielectric constant and loss were measured using an HP 4284A (Agilent, Palo Alto, CA) at 0.1, 1, 10, and 100 kHz from 150 °C down to −60 °C. The breakdown measurements were made using a Hipot tester (QuadTech, Maynard, MA) at 100 V/s. Energy density at room temperature was determined using a discharge circuit with calibrated resistors, measured with an Agilent 54622A (Agilent, Palo Alto, CA) oscilloscope while integrating the resultant curve.

Slices from each of the various samples were mounted in epoxy and polished from 600 grit SiC carbide to 0.05 μm Al_2O_3. The epoxy mounts were carbon coated and masked with conductive tape for Scanning Electron Microscopy (SEM). Images of the polished surfaces were obtained using a NOVA 600 dual beam Focused Ion Beam (FIB) system (FEI Company, The Netherlands).

3 Results and discussion

Table 1 shows the different compositions that have been successfully synthesized in the current study in contrast to compositions from the previous NRL study. Barium

Table 1 Sample composition in mol.%.

	BT (Previous study[6])	BST 50/50	BST 70/30	BST 80/20
BaO	36.7	19.34	28.62	35.01
SrO	–	19.34	12.27	8.75
TiO_2	32.4	31.32	33.11	35.43
SiO_2	14.2	17.14	14.28	11.32
Al_2O_3	14.8	12.86	10.72	8.48
BaF_2	0.6	–	1	1
MgO	1.3	–	–	–

Titanate (BT) was made earlier, while the new study concentrates on creating barium strontium titanate. (BST 50/50 is $Ba_{0.5}Sr_{0.5}TiO_3$) In both cases the glass content was intentionally low to maximize the contribution of the ferroelectric ceramic to the dielectric constant.

It is important to note that the BST samples contained Al_2O_3, as this addition played a key role in obtaining BST as the primary crystalline phase. Figure 1 illustrates XRD data of BST 80/20 samples showing that without the addition of alumina (Fig. 1(a)) the sample contained approximately 50% BST, while the other half was a crystalline silicate phase. Then, with only a small addition of alumina the dominant phase is BST with some remnant silica. A small amount of barium-rich phase also exists that is unidentified in the spectra, but is either unreacted BaO or $BaSiO_3$. The need for Al_2O_3 to form the proper phases was consistent for all compositions that were tested and can be explained by the work of Herczog et al. which showed that alumina acts as a network former. In the correct ratio with silica, alumina prevents high cross-linking of the Ti^{4+} ions in barium titanate glass-ceramics so that a stable random network forms [14, 15]. In addition, by keeping the silica content low, the glass network breaks down easily, which promotes the nucleation of the crystalline phase and keeps the starting grain size small [16]. This is ideal because a reasonable dielectric constant can be achieved when the amount of remnant silica is low.

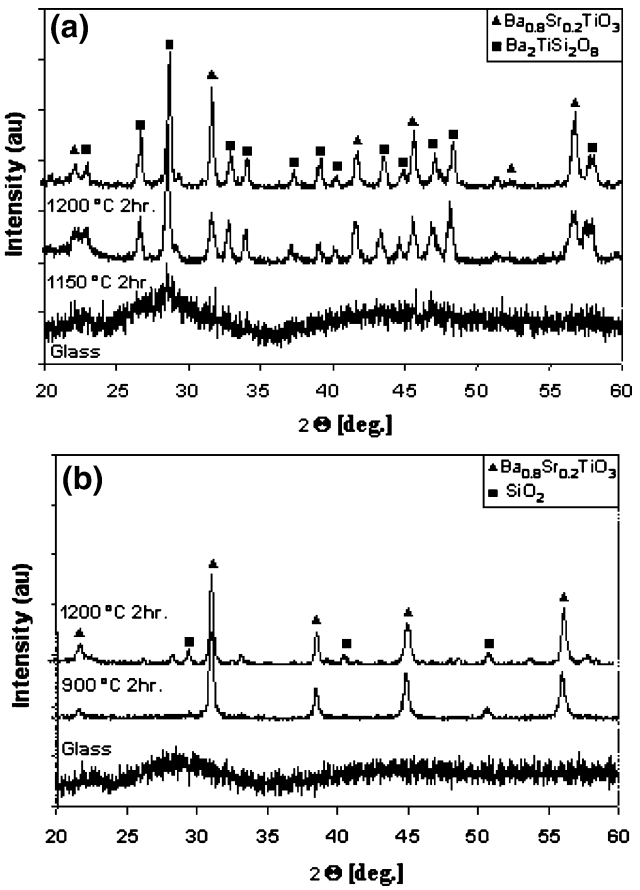

Fig. 1 XRD spectra of $Ba_{0.8}Sr_{0.2}TiO_3$ with (**a**) no Al_2O_3 and (**b**) a small Al_2O_3 addition

Once samples contained the desired crystalline phase, dielectric property and energy density measurements were taken. Figure 2 shows the effect that composition has on the dielectric constant and Curie temperature. The BST 50/50 sample exhibits a peak dielectric constant of 250 at −90 °C, while BST 80/20 has a peak dielectric constant of 1000 at 80 °C. Consequently, as more SrO is added the Curie temperature and room temperature dielectric constant decreases, which contradicts values from traditionally prepared ceramic BST samples [17]. However, the dielectric constant in BST 50/50 is decreased due to the higher glass content needed to create the initial melt because of the higher melting point of $SrTiO_3$. For example, 30 mol.% glass constituents was required for BST 50/50 while only 20 mol.% glass was needed for BST 80/20. Consequently, this study shows that a dielectric constant of 1000 can be obtained as compared to the barium titanate study where the highest dielectric constant was 350. Additionally, the dielectric loss for the BST glass-ceramic samples was ≤0.04 with most values less than 0.01. This is promising as most applications for capacitors require low loss and good thermal management.

The breakdown strength of these samples also varied. As the barium content increased, the breakdown strength decreased. BST 50/50 had breakdown strength of 800 kV/

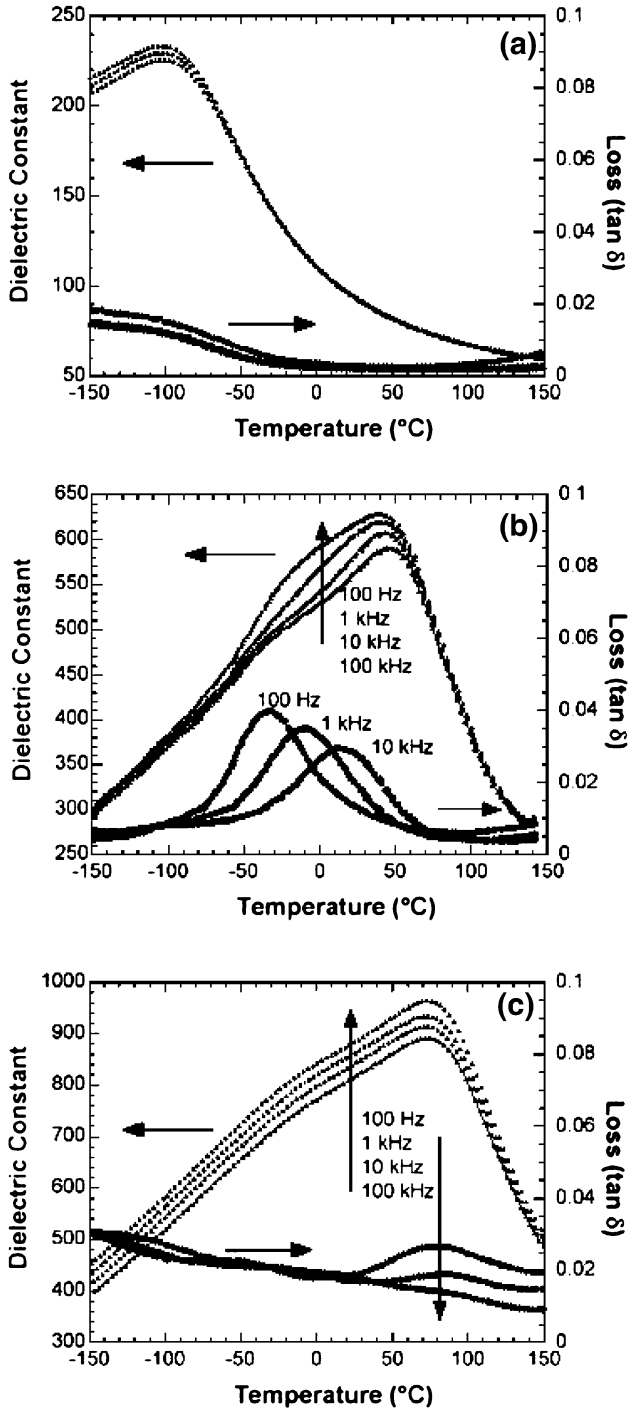

Fig. 2 Dielectric constant and loss versus temperature for BST (**a**) 50/50, (**b**) 70/30, (**c**) 80/20 annealed at 1200°C for 10 h

cm, BST 70/30 was 500 kV/cm, and BST 80/20 was 300 kV/cm. The same trend occurred in the resulting energy density, where BST 50/50 had the highest storage capacity. The values ranged from 0.9 J/cm^3 for BST 50/50 to 0.3 J/cm^3 for the BST 80/20 sample. In terms of the breakdown strength, the obtained values were nearly one order of magnitude higher than typical ceramic BST values due to the glassy matrix phase. The energy density though is much lower than anticipated, because a dielectric constant of 1000 and breakdown strength of 300 kV/cm should provide values

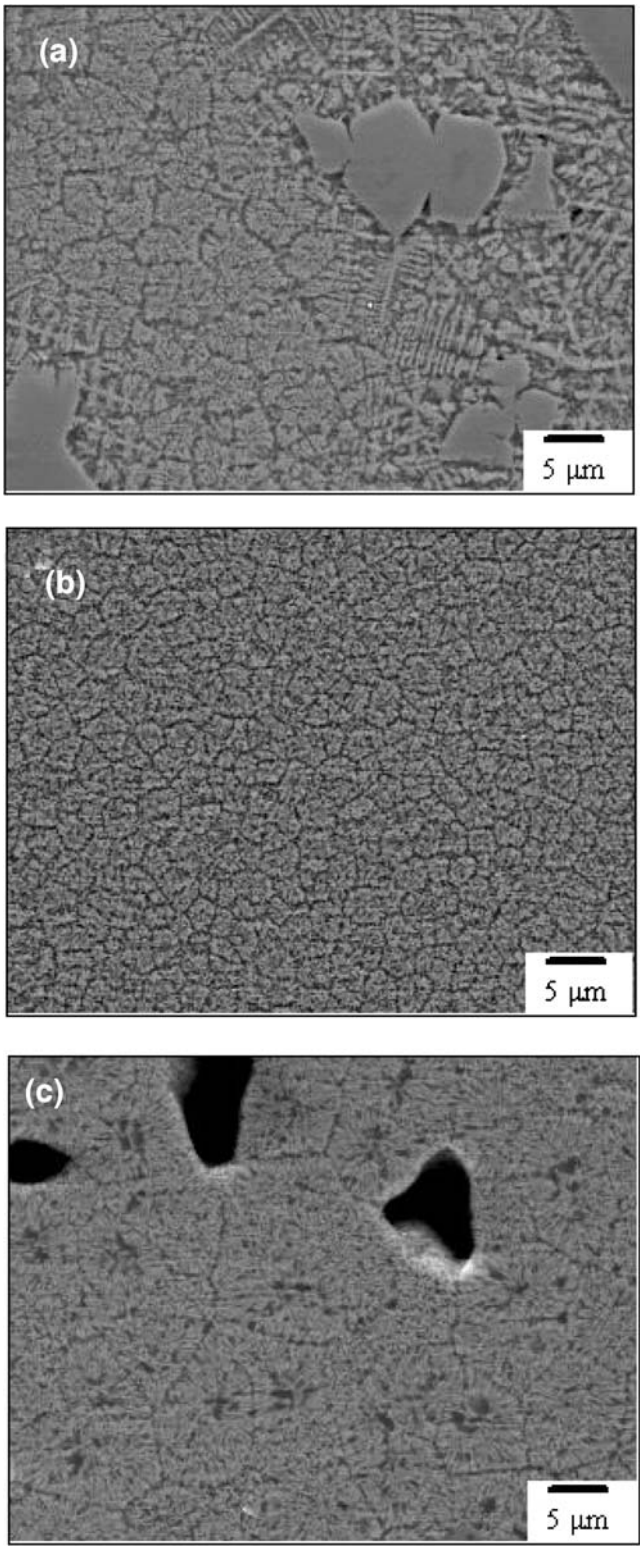

Fig. 3 SEM micrographs of BST (**a**) 50/50, (**b**) 70/30, and (**c**) 80/20 showing the presence of dendrite and pores

of 5–10 J/cm^3. Though these values were disappointing, the potential to achieve 10 J/cm^3 still exists as these samples were not completely optimized. The SEM images of the BST samples could offer a potential explanation (Fig. 3). The microstructures contain several types of dendrites, which may create a high field concentration at the tips of the dendrites causing premature failure. As the barium to strontium ratio increased, the dendrites had a finer structure and began to resemble more leaf-like or seaweed-like dendrites. Dendrite formation in glass-ceramic systems has been reported before, and in all cases has been deleterious to the desired properties [18, 19]. The samples also contain pores, which reduces the dielectric properties showing the need for optimization of processing conditions.

In order to prevent the formation of dendrites, many processing parameters can be adjusted. For example, the cooling rate of the glass can be increased or refining agents can be added to the melt. Additionally, B_2O_3 could be used as a glass former instead of SiO_2 to reduce the viscosity of the melt to allow for higher diffusivity of the constituent elements. In this study, various refining agents were tested to achieve better energy density values through microstructure refinement. Fluorine (BaF_2, due to reduced volatility over elemental fluorine) was added to increase the dielectric constant as was reported in previous studies of barium titanate ceramics [20]. In this case the fluorine addition had several positive effects. Figure 4(a) shows that 1 mol.% fluorine in a BST 80/20 sample drastically modifies the microstructure when compared to Fig. 3(c). The barium fluoride addition eliminated the porosity and produced distinctive cubic grains instead of the previous dendritic structure. The fluorine appeared to homogenize the composition to avoid local supersaturation of any constituents so that dendrites do not form. Figure 4(b) shows the homogenization as the XRD spectra of the sample containing fluorine only has BST and remnant silica, whereas the sample without fluorine contains other barium-rich phases that are BaO or $BaSiO_3$. The addition of fluorine had similar results for all BST stoichiometries that were tested.

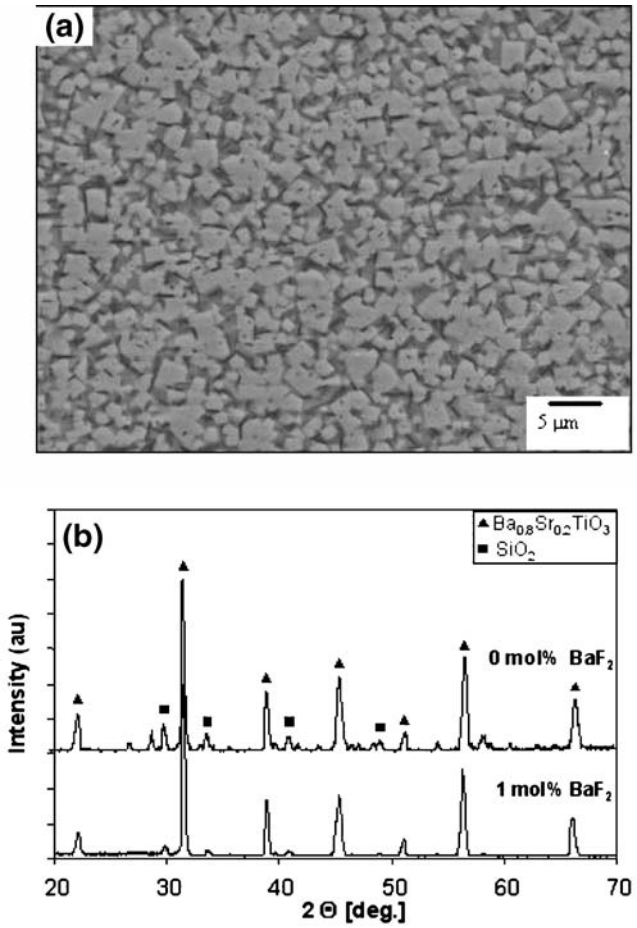

Fig. 4 (**a**) SEM micrograph and (**b**) XRD spectra of BST 80/20 annealed at 1200°C for 10 h with 1 mol.% BaF_2 showing the effect of fluorine addition on homogenizing the composition and microstructure

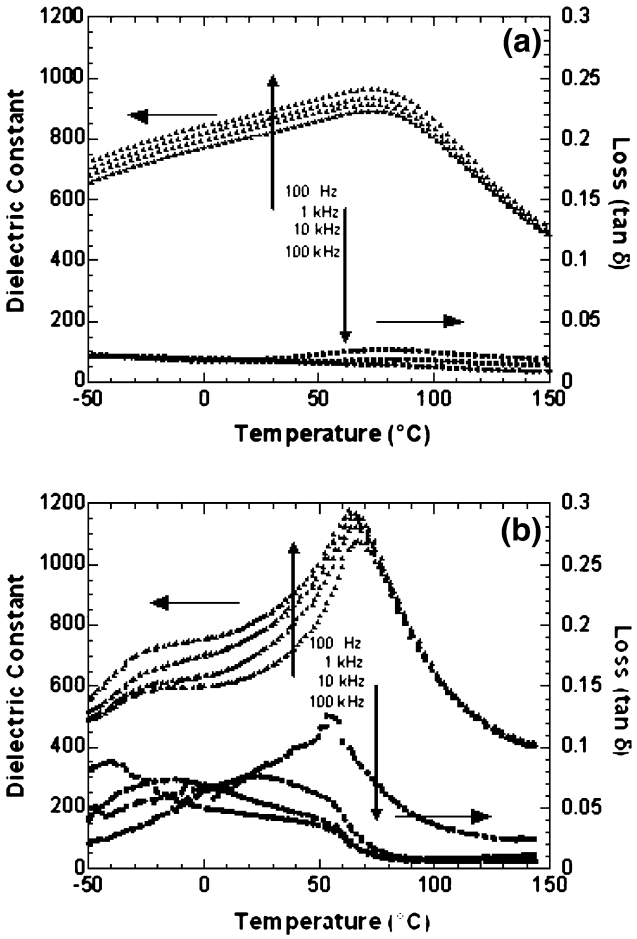

Fig. 5 Dielectric constant versus temperature plots for BST 80/20 annealed at 1200°C for 10 h with (**a**) 0 mol.% BaF_2 and (**b**) 1 mol.% BaF_2 showing that the fluorine addition also enhances the dielectric response

The measurements of the lattice parameter from the XRD data further supports this argument as the fluorine sample equates to $Ba_{0.783}Sr_{0.21}TiO_3$ composition whereas the sample without fluorine equates to $Ba_{0.55}Sr_{0.45}TiO_3$. In fact other compositions without fluorine did not have the anticipated composition, i.e. BST 50 was $Ba_{0.42}Sr_{0.58}TiO_3$. This suggests that the barium-rich phases that form without the fluorine is at the expense of forming the correct BST phase and reduces the overall properties. In addition, the removal of porosity has also altered the properties. Since fluorine decreases the viscosity of the glass melt, bubbles escape more easily. This leads to fewer bubbles in the melt, thus reducing the amount of porosity in the final glass ceramic. Figure 5 compares the dielectric properties of BST 80/20 with 0 and 1 mol.% BaF_2. With the addition of barium fluoride the dielectric response is closer to that of a BST 80/20 ceramic. Two peaks in the dielectric constant are evident corresponding to the phase transformations that occur in BST, and the dielectric constant peaks are sharp as would be expected from a normal ferroelectric material. The peak dielectric constant did not increase dramatically, but this was expected as 20–30% remnant glass exists in the BST glass-ceramics. On the other hand, the sample without barium fluoride has a flat dielectric constant response, which is most likely related to the excess crystalline silica and the heterogeneous microstructure. Interestingly, the Curie point shifts to a slightly lower temperature with the incorporation of fluorine while the dielectric loss increases slightly. The dielectric loss may pose a problem in certain applications, but other additives may be able to reduce the loss in these circumstances. For the purpose of this study, the dielectric loss is not an issue.

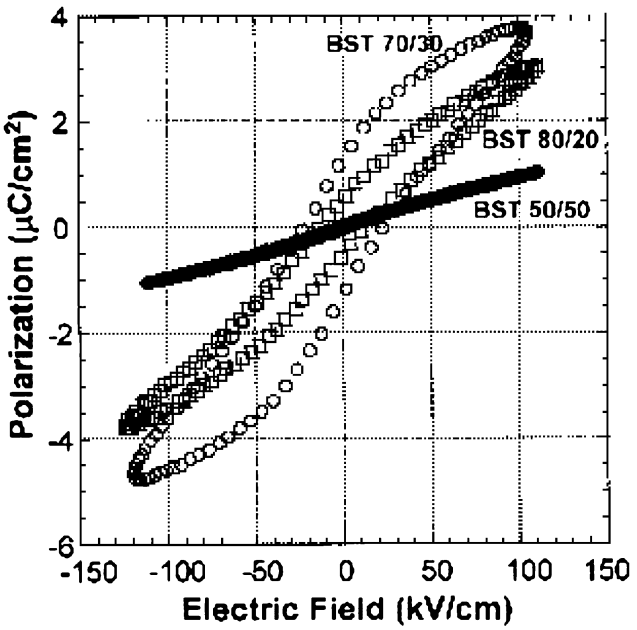

Fig. 6 Polarization versus electric field plot showing the hysteresis behavior of various BST contents at low field

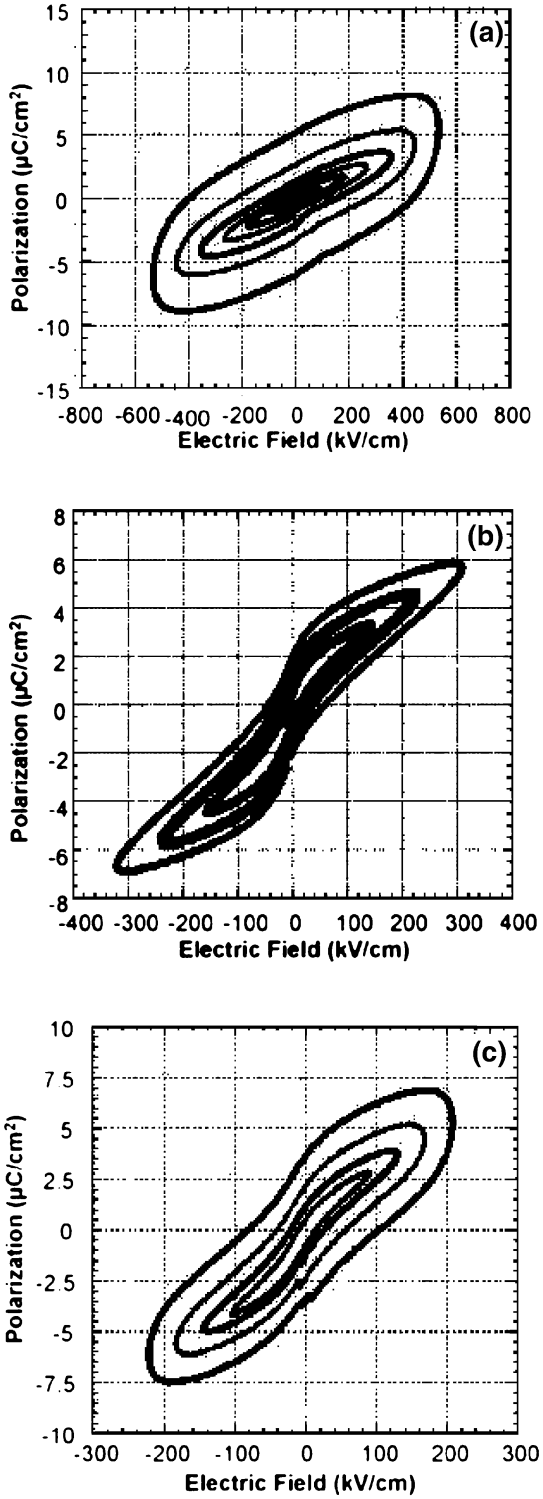

Fig. 7 Polarization versus electric field plot showing the dramatic increase in hysteresis with increased field for (**a**) BST 50/50, (**b**) BST 70/30, and (**c**) BST 80/20 annealed at 1200°C for 2 h

Though the dielectric constant changed only slightly with the addition of fluorine, the energy density dramatically

increased. In the case of BST 80/20 annealed at 1200 °C for 2 h the energy density was 0.28 J/cm^3 before the addition and 0.5 J/cm^3 after the fluorine addition. The increase in energy density was partially due to the fact that the samples could be driven to higher field, which is evident by the increase in the breakdown strength. The breakdown strength of BST 80/20 annealed at 1200 °C for 2 h was 300 kV/cm before the addition and 550 kV/cm after the fluorine addition. The overall increase in the breakdown strength is most likely due to the reduction of pores and dendrites. This suggests that improving the microstructure can eliminate field concentrations, and increase the overall energy storage, but the relative negative contribution of dendrites to pores cannot be separated.

In addition to the discharge measurements, Polarization versus electric field was measured for the glass-ceramic samples and used to verify the energy density results. The energy density was obtained by integrating the area between the polarization axis and the discharge curve in a polarization versus electric field plot. The resultant energy densities were closely matched to those obtained using the discharge circuit for all samples tested. Figure 6 shows an example of the polarization versus electric field plots for BST 50/50, 70/30, and 80/20 samples. These samples were driven at low fields to show the generic behavior and do not show the breakdown strength of the materials. The BST 50/50 sample exhibits a linear dielectric response as the samples were tested at room temperature where the sample is well into the paraelectric regime. Both the BST 70/30 and 80/20 samples showed ferroelectric behavior as would be expected at room temperature. Since the dielectric constant is defined as the slope of the polarization curve, it makes sense that the BST 50/50 sample has the lowest slope. The BST 70/30 and 80/20 samples have nearly the same slope at zero field, which is confirmed by Fig. 2 showing the room temperature dielectric constant was approximately the same.

There appears to be a large amount of hysteresis in BST 70/30 and 80/20 specimens that may be attributed to the glassy phase. However, Fig. 7 shows that the hysteresis in all BST samples increases tremendously with the increase of field. This phenomenon is believed to be due to interfacial polarization. Since the dielectric constant and the conductivity of the glass and ceramic phase is so vastly different, charge tends to build up at the interface and become trapped in the sample. This interfacial polarization may be the cause of the hysteresis and thus contribute to the low energy density values. To better understand the issue of interfacial polarization a computation and modeling study is underway and the results will be reported at a later date [21].

Additionally, future studies plan to observe what effects other refining agents such as B_2O_3 and LiF have on BST glass-ceramics as well as more fully understand the kinetics and phase formation of the ceramic components in this system.

4 Conclusions

In this study it was determined that Al_2O_3 was the key to forming the BST phase as only crystalline silicate phases were formed without the addition. It was found that a dielectric constant of 1000 and a breakdown strength of 800 kV/cm could be achieved. In this study, energy density was measured in two ways as opposed to incorrectly projecting a value from linear dielectric behavior. Though the dielectric constant and breakdown strength were improved, the energy density was only 0.3–0.9 J/cm^3. These values were lower than anticipated due to the presence of dendrites and pores in the microstructure. When BaF_2 was added as a refining agent the microstructure improved and the energy density doubled for the BST 80/20 samples. No refining agent that was added could reduce the amount of hysteresis that developed when increasing electric field was applied to the samples. This hysteresis is believed to be due to interfacial polarization and will be the focus of future studies.

Acknowledgments This research was performed while the author held a National Research Council Research Associateship Award at the U.S. Naval Research Laboratory. The authors would also like to acknowledge funding from the Office of Naval Research under contract #N0001404WX20802.

References

1. R. O'Rourke, *Electric drive propulsion for U.S. navy ships: background and issues for congress* (CRS Resport # RL30622, July 31, 2000)
2. B.J. Baliga, Proc. IEEE **89**(6), 822–832 (2001)
3. W.J. Sarjeant, I.W. Clelland, R.A. Price, Proc. IEEE **89**(6), 846–855 (2001)
4. A.J. Moulson, J.M. Herbert, *Electroceramics*, Chapter 5. (Wiley, Chichester, England, 2003)
5. J.R. Laghari, W.J. Sarjeant, IEEE Trans. Power Electron. **7**(1), 251–257 (1992)
6. M.-J. Pan, R.J. Rayne, B.A. Bender, M. Lanagan, *Proceedings of the 2004 ASNE Electric Machines Technology Symposium* (Philadelphia, PA, January 27–29, 2004)
7. R. Gerson, T.C. Marshall, J. Appl. Physi. **30**(11), 1650–1653 (1959)
8. A. Herczog, IEEE Trans. Parts Hybrids and Packag. **9**(4), 247–256 (1973)
9. P.W. McMillian, *Glass-ceramics* (Academic, New York, 1964)
10. S.D. Stookey, Ind. Eng. Chem. **51**(7), 805–808 (1959)
11. S.L. Swartz, *Dielectric Properties of Strontium Titanate Glass Ceramics*, Ph. D. Thesis, The Pennsylvania State University, (1985)
12. M.-J. Pan, M. Lanagan, B.A. Bender, C.-T. Cheng, Ceramic Transactions, in *Synthesis, Properties, and Crystal Chemistry of Perovskite-based Material*, vol. 169, ed. by A. Goyal (American Ceramic Society, Westerville, OH, 2005), pp. 187–194

13. N.H. Fletcher, A.D. Hilton, B.W. Ricketts, J. Phys. D: Appl. Phys. **29**(1), 253–258 (1996)
14. A. Herczog, S.D. Stookey, French Patent 1272036 (1961)
15. A. Herczog, J. Am. Ceram. Soc. **47**(3), 107–115 (1964)
16. M.M. Layton, A. Herczog, Glass Technol. **10**(2), 50–53 (1969)
17. A.D. Hilton, B.W. Ricketts, J. Phys. D: Appl. Phys. **29**(5), 1321–1325 (1996)
18. J.-J. Shyu, J.-R. Wang, J. Am. Ceram. Soc. **83**(12), 3135–3140 (2000)
19. Q.A. Juma'a, J.M. Parker, Advances in Ceramics, in *Nucleation and Crystallization in Glasses*, vol. 4, ed. by J.H. Simmons, D.R. Uhlmann, G.H. Beall (American Ceramic Society, Westerville, OH, 1982), pp. 218–236
20. G. Partridge, Adv. Mater. **4**(10), 668–673 (1992)
21. M.-J. Pan, E. Gorzkowski, J. Am. Ceram. Soc. (in review)